THE JOURNAL OF BIOLOGICAL CHEMISTRY VOL. 287, NO. 11, pp. 8242–8253, March 9, 2012

Ca^{2+}-dependent GTPase, Extra-large G Protein 2 (XLG2), Promotes Activation of DNA-binding Protein Related to Vernalization 1 (RTV1), Leading to Activation of Floral Integrator Genes and Early Flowering in *Arabidopsis*[*S]

Received for publication, November 7, 2011, and in revised form, December 20, 2011 Published, JBC Papers in Press, January 9, 2012, DOI 10.1074/jbc.M111.317412

Jae Bok Heo[‡§¶‖], **Sibum Sung**[§], **and Sarah M. Assmann**[‡1]

From the [‡]*Department of Biology, Penn State University, University Park, Pennsylvania 16802, the* [§]*Section of Molecular Cell and Developmental Biology and Institute for Cellular and Molecular Biology, University of Texas, Austin, Texas 78712, and the* [¶]*Department of Molecular Biotechnology and the* [‖]*BK21 Center for Silver-Bio Industrialization, Dong-A University, Busan 604-714, Korea*

Background: Extra-large G proteins, XLGs, are nuclear GTP-binding proteins with both Gα-like and novel domains.
Results: Unlike general G proteins, XLG proteins are Ca^{2+}-dependent GTPases, and XLG2 interacts with the nuclear protein RTV1 (related to vernalization 1).
Conclusion: GTP-bound XLG2 promotes RTV1-chromatin interaction, leading to activation of floral integrator genes.
Significance: XLGs unusually integrate Ca^{2+}-based and G protein-based cellular pathways and control flowering.

Heterotrimeric G proteins, consisting of Gα, Gβ, and Gγ subunits, play important roles in plant development and cell signaling. In *Arabidopsis*, in addition to one prototypical G protein α subunit, GPA1, there are three extra-large G proteins, XLG1, XLG2, and XLG3, of largely unknown function. Each extra-large G (XLG) protein has a C-terminal Gα-like region and a ~400 amino acid N-terminal extension. Here we show that the three XLG proteins specifically bind and hydrolyze GTP, despite the fact that these plant-specific proteins lack key conserved amino acid residues important for GTP binding and hydrolysis of GTP in mammalian Gα proteins. Moreover, unlike other known Gα proteins, these activities require Ca^{2+} instead of Mg^{2+} as a cofactor. Yeast two-hybrid library screening and *in vitro* protein pull-down assays revealed that XLG2 interacts with the nuclear protein RTV1 (related to vernalization 1). Electrophoretic mobility shift assays show that RTV1 binds to DNA *in vitro* in a non-sequence-specific manner and that GTP-bound XLG2 promotes the DNA binding activity of RTV1. Overexpression of RTV1 results in early flowering. Combined overexpression of XLG2 and RTV1 enhances this early flowering phenotype and elevates expression of the floral pathway integrator genes, *FT* and *SOC1*, but does not repress expression of the floral repressor, *FLC*. Chromatin immunoprecipitation assays show that XLG2 increases RTV1 binding to *FT* and *SOC1* promoters. Thus, a Ca^{2+}-dependent G protein, XLG2, promotes RTV1 DNA binding activity for a subset of floral integrator genes and contributes to floral transition.

Signaling via heterotrimeric G proteins, composed of Gα, Gβ, and Gγ subunits, is highly conserved in eukaryotes (1–4). Classically, G protein-mediated signaling is initiated by ligand binding to a cell surface G protein-coupled receptor, which has seven transmembrane domains. Ligand binding activates receptor-mediated GDP/GTP exchange on the Gα subunit. Resultant GTP binding causes the dissociation of Gα from the Gβγ dimer, and the activated Gα and Gβγ interact with downstream target proteins, leading to numerous cellular responses (5–7). Although mammals have 800–1000 protein-coupled receptors, 23 Gα, 5 Gβ, and 12 Gγ subunits (8), plants have a greatly reduced number of heterotrimeric G protein signaling elements (9–11). For instance, the *Arabidopsis* genome encodes only one Gα subunit (GPA1), one Gβ subunit (AGB1), three Gγ subunits (AGG1, AGG2, and AGG3), and 1–2 dozen candidate G protein-coupled receptors (12–18). However, despite the small number of heterotrimeric G protein signaling elements, heterotrimeric G proteins play important roles in many physiological and developmental processes in plants (3, 10, 19).

Besides the canonical Gα subunit gene, *GPA1*, there are three genes in *Arabidopsis* that encode unusual extra-large GTP-binding proteins, known as XLGs (20, 21). All XLG proteins have C-terminal Gα domains that are homologous to GPA1 and other Gα subunits. The unique N-terminal regions of XLGs consist of ~400 amino acid sequences that are highly conserved among the XLG proteins. XLG proteins appear to be unique to the plant kingdom and are not homologous to the XLαs of mammals (21). Despite variations in conserved amino acid residues required for GTP binding compared with canonical Gα proteins, recombinant XLG1 protein was previously shown to bind GTP, which is a functional characteristic of Gα proteins (20). Loss-of-function analyses showed redundancy in XLG function; dark-grown *xlg1-1 xlg2-1 xlg3-1* triple mutant plants show an increased primary root length and altered sensitivity in root growth in response to sugar, abscisic acid, osmotic stress,

* This research was supported by United States Department of Agriculture Grant 2003-35304-13924 and Penn State funding (to S. M. A.), by National Science Foundation Grant IOS 0950785 (to S. S.), and Next-Generation BioGreen 21 Program SSAC Grant PJ008087 and a National Research Foundation of Korea Grant funded by the Korean Government (MEST Grant 2011-0013137) (to J. B. H.).
[S] This article contains supplemental Table 1 and Figs. 1–6.
[1] To whom correspondence should be addressed: Dept. of Biology, 208 Mueller Laboratory, Penn State University, University Park, Pennsylvania 16802. Tel.: 814-863-9579; Fax: 814-865-9131; E-mail: sma3@psu.edu.

and ethylene. In addition, XLG3 is specifically involved in the regulation of root waving and skewing (21, 22), and XLG2 interacts with the sole *Arabidopsis* canonical Gβ subunit, AGB1, and is involved in pathogen resistance (23). Expression analyses of *XLG* genes using RT-PCR and a reporter gene assay show that all three XLGs are widely expressed throughout the plant, suggesting that XLGs may have additional functions in plant development and signaling beyond those already reported (21).

In *Arabidopsis*, flowering time is controlled by multiple endogenous and environmental cues, including photoperiod, temperature, and gibberellins. Floral regulatory cues are integrated by a group of genes, including *FT* (flowering locus T), *SOC1/AGL20* (suppressor of overexpression of constans 1), *AGL24* (agamous-like 24), and *LFY* (leafy). These genes are often referred to as "floral integrators" because most known flowering pathways eventually regulate expression of these flowering genes (24–27). Studies in *Arabidopsis* and rice have shown that the floral integrator FT is a major component of florigen (28, 29). FT together with FD (flowering locus D) activates *SOC1* in the meristem (30). Floral integrators, in turn, activate floral meristem identity genes, including *AP1* (apetala 1) and *FUL* (fruitful) (30, 31). Thus, there is an intricate regulatory network among floral integrators and floral meristem identity genes to initiate and maintain floral transition in response to endogenous and environmental cues (24, 25, 27, 30, 31).

Winter annual strains of *Arabidopsis* contain functional *FRI* (frigida) and *FLC* (flowering locus C) genes and flower extremely late unless plants are exposed to a prolonged period of cold (*i.e.* vernalization). *FLC* acts as a potent floral repressor by the direct suppression of floral regulators *FT* and *SOC1* (32, 33). Vernalization results in stable repression of *FLC* to allow rapid flowering (34). Similar to winter annual strains of *Arabidopsis*, a group of late flowering mutants flower late in an *FLC*-dependent manner (35). These mutants are collectively referred as the autonomous pathway mutants, and vernalization results in rapid flowering in the autonomous mutants as well (35). Vernalization results in an increase in two repressive histone modifications of *FLC* chromatin: methylation of histone H3 Lys-9 and histone H3 Lys-27 (34, 36). These vernalization-induced histone modifications are mediated by a number of proteins, including VRN2 (vernalization 2), VRN1 (vernalization 1), and VIN3 (vernalization-insensitive 3) (34, 36). In this study, we describe the biochemical characterization of the XLG2 protein and address its function in regulation of RTV1 (related to vernalization 1) and in floral transition, thereby elucidating a role of this unusual G protein in the control of flowering time.

EXPERIMENTAL PROCEDURES

Plant Materials and Vernalization Treatment—Seeds were germinated on 0.8% agar plates with half-strength Murashige and Skoog salt, 0.8% sucrose, stratified at 4 °C for 2 days, and grown for 10 days in long day conditions (16 h of light at 22 °C, and 8 h of dark at 22 °C) or short day conditions (8 h of light at 22 °C, 16 h of dark at 22 °C), and then plants were transplanted to soil or harvested for RNA isolation. Light intensity for LD[2] and SD conditions was ~70 μmol m^{-2} s^{-1}. For the vernalization treatment, seeds were germinated on agar plates for 5 days in SD conditions, and vernalized for 5 weeks at 4 °C in SD (37), and then plants were harvested for RNA isolation, or plants were transplanted to soil and transferred to growth chambers (21 ± 2 °C) under LD or SD conditions for flowering time tests.

Protein Expression in Escherichia coli and Generation of XLG2(T475N) Mutant Construct—For expression in *E. coli*, the coding regions of the *XLG* genes and *GPA1* cDNA were subcloned into the pET28a-modified expression vector (Novagen) which results in production of fusion proteins with N-terminal His_6 and thioredoxin (TRX) tags. We fused XLG proteins with TRX to increase solubility of the recombinant proteins. The coding region of *RTV1* and each *XLG* was also subcloned into the pGEX-2T vector, which produces GST fusion proteins. XLG C-terminal regions (amino acids 486–888 for XLG1, 461–862 for XLG2, and 433–849 for XLG3) were also subcloned into the same vector. All constructs were transformed into the *E. coli* BL21(DE3)pLysS strain. Transformed cells were inoculated into 10 ml of LB medium containing 25 μg/ml kanamycin for pET28a and 50 μg/ml ampicilin for pGEX-2T. The cultures were grown at 30 °C overnight and then poured into 500 ml of fresh LB medium. When an A_{600} of 0.8 was reached, isopropyl β-D-thiogalactopyranoside was added to the cultures to a final concentration of 0.9 mM, and the incubation was continued for another 4 h at 30 °C for induction. His-tagged fusion proteins were purified using Ni^{2+}-nitrilotriacetic acid-agarose column chromatography (Qiagen) (supplemental Fig. 1, *a* and *b*), and GST fusion proteins were purified using glutathione-agarose (Sigma) according to each manufacturer's instructions. Empty vectors were transformed into the *E. coli* BL21 (DE3) pLysS strain and expressed for purification of His_6 TRX or GST. To purify XLG proteins lacking any tag, GST was cleaved by thrombin (Sigma) from GST fusion XLG proteins. Mutant (T475N) forms of full-length XLG2 and XLG2C were constructed by PCR using the following primers: 5′-GGTGGCGCCAATACAATTTACAAA-3′ and 5′-TTTGTAAATTGTATTGGCGCCACC-3′.

GTP Binding Assay—The [^{35}S]GTPγS binding activity of full length XLGs, C-terminal regions of the XLGs, GPA1, and TRX protein was measured by the rapid filtration method (38, 39). A 100 nM concentration of each purified recombinant proteins was incubated at 30 °C in 200 μl of 50 mM Tris-Cl buffer, pH 8.0, containing 1 mM EDTA, 1 mM dithiothreitol (DTT), 1 mM NaN_3, 0.2 μM [^{35}S]GTPγS, and 10 mM $MgCl_2$ or $CaCl_2$. The reaction was stopped by the addition of 2 ml of ice-cold buffer (20 mM Tris-Cl, pH 8.0, 100 mM NaCl, and 25 mM $MgCl_2$). Aliquots (20 μl) were taken at the indicated times and vacuum-filtered onto nitrocellulose membranes (Millipore, Billerica, MA), which had been rinsed with 3 ml of ice-cold buffer, and membrane-bound material was washed rapidly three times

[2] The abbreviations used are: LD, long day; SD, short day; GUS, β-glucuronidase; TRX, thioredoxin; GAP, GTPase-activating protein; GTPγS, guanosine 5′-3-*O*-(thio)triphosphate; SC, synthetic complete; NLS, nuclear localization signal.

with 3 ml of ice-cold buffer. The washed membranes were dried and quantified for radioactivity by liquid scintillation counting.

GTPase Assay—GTP hydrolysis assays were performed as previously described (40) using PEI-cellulose TLC plates. Briefly, the reaction was performed at 30 °C in 200 μl of buffer containing 50 mM Tris-Cl, pH 8.0, 1 mM EDTA, 1 mM dithiothreitol, 1 mM NaN_3, 20 pmol of [α-^{32}P]GTP, 100 nM full-length or C-terminal XLG protein or 100 nM of GPA1 protein, and 10 mM $MgCl_2$, $MnCl_2$ or $CaCl_2$. Aliquots of 10 μl were sampled at appropriate time intervals, and 10 μl of 0.5 M EDTA (pH 8.0) was added to the aliquots to stop the reaction. Samples (2 μl) were spotted onto PEI-cellulose TLC plates, which were then developed in 0.5 M KH_2PO_4, pH 3.4, solution. After drying, the plates were exposed to a storage phosphor screen (Amersham Biosciences) and then scanned by a PhosphorImager (GE Healthcare).

Yeast Two-hybrid Screening—Yeast two-hybrid screening was carried out according to the manufacturer's protocol (Clontech). Briefly, the bait plasmid, pBUTE-XLG2, and total cDNAs of *Arabidopsis* obtained from ABRC (catalogue number CD4-10) in which the cDNAs were fused to the pACT-AD were used sequentially to transform *Saccharomyces cerevisiae* strain pJG69-4A. The resulting transformants were then plated on synthetic complete (SC) medium lacking uracil (Ura), leucine (Leu), and histidine (His) (SC−, Ura$^-$, Leu$^-$, and His$^-$) and/or SC− Ura$^-$ and Leu$^-$, including 3 mM 3-aminotriazole. Histidine-positive colonies were further tested for β-galactosidase (*LacZ*) activity according to the manufacturer's protocol (Clontech). The clones of cDNAs encoding candidate XLG2 interacting proteins were selected and isolated based on their growth as blue colonies in histidine-deficient medium. The cDNAs were isolated and sequenced. The DNA sequences were then subjected to BLAST analysis using the GenBank™ database.

In Vitro Protein Pull-down Assay—Purified GST or GST-RTV1 was incubated for 2 h at 4 °C with 40 μl of glutathione-Sepharose in PBST (PBS containing 1% Triton X-100). After three washes, the beads were incubated with His-XLG2C in 0.5 ml of PBST for 3 h on a rotary shaker at 4 °C. The beads were then washed five times with PBST, boiled with SDS sample buffer, and subjected to 12% SDS-PAGE. Western blot of the resolved proteins was carried out using anti-His (Qiagen catalog no. 34660) and anti-GST (Novagen catalog no. 71097) monoclonal antibodies.

Transient Expression Proteins Fused with Green Fluorescent Protein—RTV1 cDNA was fused upstream of the GFP cDNA under the control of the CaMV 35S promoter (pUC::GFP) (41). The construct (*RTV1-GFP*) was co-transformed into *Arabidopsis* protoplasts along with the red fluorescent protein cDNA fused to a nuclear localization signal peptide (*NLS-RFP* (42)). Transient expression of GFP- and RFP-fused constructs in *Arabidopsis* protoplasts was performed according to the method described by Heo *et al.* (40). Briefly, recombinant plasmids were introduced by polyethylene glycol (PEG)-mediated transformation into *Arabidopsis* protoplasts that had been prepared from leaf tissues. Expression of the fusion constructs was monitored after transformation and observed by fluorescence microscopy (Olympus AX70 TR, Olympus).

Production of Transgenic Arabidopsis Lines—For generation of P_{RTV1}::GUS lines (Col background), the *RTV1* promoter (0.91 kb, which is the complete intergenic region) was amplified and subcloned into the pENTR directional TOPO vector (Invitrogen) followed by LR reaction (Invitrogen) into the destination vector pHGWFS7 (43) using LR enzyme (Invitrogen). GUS activity was revealed by incubation in 100 mM $NaPO_4$ (pH 7.2), 2.5 mM 5-bromo-4-chloro-3-indoyl-β-D-glucuronide. Plant tissue was incubated at 37 °C for 24 h. After staining, chlorophyll was cleared from the samples by dehydration using 70% ethanol.

To generate 35S-RTV1 lines, RTV1 cDNA was ligated to the pH7GWIWG2 vector, and the construct was transformed into wild-type plants (Col-0) via *Agrobacterium*-mediated transformation (44). For 35S-XLG2 RTV1, XLG2 cDNA was ligated to pGWB11, and the resulting 35S-XLG2 construct was transformed into the T1 generation of *35S-RTV1(13)* plants. Transgenic lines were selected on selective antibiotic marker-containing medium and were confirmed by genotyping PCR. To generate *35S-RTV1-GFP ft-1* lines, the *35S-RTV1-GFP* construct was transformed into *ft* mutant plants by floral dipping, and then T1 generation plants were selected by selective antibiotic-containing medium, followed by flowering time determination.

Electrophoretic Mobility Shift Assay (EMSA)—EMSAs were performed as described by Despres *et al.* (45). DNA fragments of *FLC*, *SOC1*, *FT*, *VRN2*, and *DFR* promoters 400 bp upstream of their start codons were generated by PCR amplification and confirmed by sequencing. 100 ng of double-stranded synthetic nucleotides were radiolabeled using T4 polynucleotide kinase. EMSA reactions were performed at room temperature for 30 min in 15 μl of EMSA buffer (20 mM Hepes-KOH, pH 7.9, 100 mM KCl, 2 mM DTT, and 20% glycerol) containing 1 μl (20,000 cpm) of the labeled nucleotides and 0–2 μg of RTV1. In addition, 100 nM XLG2C, 10 mM Ca^{2+}, and 1 mM GTPγS were added with the buffer in some reactions. EMSA reactions were loaded onto a 5% Tris-borate EDTA-polyacrylamide gel and run at 8 V/cm for 90 min. After electrophoresis, the gel was dried and subjected to autoradiography at −80 °C using Eastman Kodak Co. x-ray film.

Chromatin Immunoprecipitation (ChIP) Assays and Immunoprecipitation—ChIP assays were carried out (Johnson and Bresnick (46)) as described by Heo *et al.* (47), following the protocol of Gendrel *et al.* (48). Chromatin proteins and DNA were cross-linked in 10-day-old Col, *35S-RTV1(13)* and *35S-XLG2(1) RTV1* seedlings by formaldehyde fixation. Chromatin was isolated using the same extraction buffers as in Heo and Sung (47) and Gendrel *et al.* (48). Chromatin size postsonication was 500–800 bp, as confirmed by agarose gel electrophoresis (not shown). Chromatin immunoprecipitation was performed using anti-FLAG (Sigma; catalog no. F1804) or anti-GFP (Molecular Probes; catalog no. A11122) antibodies. Cross-links were reversed by incubation at 65 °C for 6 h, and DNA was purified with QIAquick spin columns (Qiagen) and eluted in 50 μl of Tris-HCl EDTA (pH 8.0). PCR was used to amplify fragments of the *FT*, *SOC1*, and *FLC* promoters as used in EMSAs. The relative -fold increase of retrieved DNAs was calculated as follows: first, relative enrichment of each fragment was calcu-

TABLE 1
Conserved nucleotide binding motifs in selected G proteins
"At" indicates *Arabidopsis thaliana*, and "Os" indicates rice (*Oryza sativa*).

Protein	G-1	G-2	G-3	G-4	G-5
Consensus	G*XXXX*GK(S/T)	*XXXTXXX*	D*X*GQ	NK*X*D	TCA
AtXLG1	GNSGSGTS	EGVTSSS	RVPSR	NKYD	SKS
AtXLG2	GSEKGGAT	EGLSSME	RLNPR	TKPD	VSL
AtXLG3	GIEGSGTS	RVRTQGN	RVNAK	NKFD	ARA
AtGPA1	GAGESGKS	RVRTTGV	DVGGQ	NKFD	TTA
OsRGA1	GAGESGKS	RVRTNGV	DVGGQ	NKFD	TTA

lated by comparison with the input (chromatin sample before immunoprecipitation). Second, the background levels of retrieved DNAs were calculated by measuring *ACTIN2* enrichment compared with input. Third, relative levels of each retrieved fragment were calculated using the formula, $C_T = C_T$(each gene) $- C_T(ACTIN2)$. Last, relative levels in Col were set equal to 1 in all cases, and -fold change relative to Col was calculated. Primers are given in supplemental Table 1.

RESULTS

GTP Binding and Hydrolytic Activities of XLG2 Protein—The C-terminal regions of XLGs contain Gα domains (G-1 to G-5) (20, 21), which, in heterotrimeric G proteins, mediate GTP binding and hydrolysis (49). However, some amino acids conserved in the G-1 to G-5 domains of Gα proteins are not conserved within the corresponding domains of XLG proteins. Particularly, amino acids in the regions of the G-3 and G-5 domains, which are involved in Mg^{2+} coordination, GTP binding, and subsequent GTP hydrolysis, are not conserved (50) (Table 1). This raised the question of whether or not XLG proteins are able to bind and hydrolyze GTP. We addressed the biochemical properties of the three XLG proteins using GTP binding and GTPase assays. Results were similar for all three XLG proteins; results for XLG2 are reported here, and those for XLG1 and XLG3 are described in supplemental Figs. 1–4. To examine specific GTPγS binding and GTPase activities, we purified and assayed recombinant GPA1 and XLG proteins fused with His_6 and TRX.

As expected, GPA1 bound GTPγS rapidly in the presence of Mg^{2+} (Fig. 1*A*), illustrating the known dependence of Gα proteins on this divalent cation (49). However, XLG2C did not bind GTPγS under these conditions (Fig. 1*A*). To address whether XLG2C has a preference for other divalent cations over Mg^{2+} for GTP binding activity, GTP binding filter assays were performed in the presence of Ca^{2+} instead of Mg^{2+}. Interestingly, the presence of Ca^{2+} promoted XLG2C binding of GTPγS, whereas in the absence of any divalent ion, there was no GTPγS binding to XLG2C (Fig. 1*B*). By contrast, GPA1 showed weaker GTPγS binding in the presence of Ca^{2+} as compared with Mg^{2+} (Fig. 1*C*). Similar to XLG2C, XLG1 and XLG3 also bound GTPγS in the presence of Ca^{2+} (supplemental Figs. 3 and 4). These results indicate that XLG proteins prefer Ca^{2+} over Mg^{2+} as a cofactor for their GTP binding activities. To confirm the specificity of GTP binding, PCR-based mutagenesis was used to generate a mutation, T475N, in the G-1 domain of XLG2, a residue which is essential for binding to the phosphate moieties of guanine nucleotides (51). Similar mutations have been reported to abolish the GTP binding activity of other G proteins. For example, the T22N mutation of rice OsRab7 protein eliminates GTP binding (52, 53). Mutations S47C of mammalian $G\alpha_o$ and S48C of $G\alpha_{i2}$ also impair GTPγS binding and create a dominant negative phenotype (54, 55). We designated this mutant protein XLG2C(T475N); this protein was also tagged with N-terminal His_6 and TRX. GTP binding by XLG2C(T475N) protein was greatly reduced (Fig. 1*C*). As expected, purified His_6 TRX control protein did not show any GTP binding activity (Fig. 1, *A* and *C*). Analogous mutations reduced the GTP binding of XLG1C and XLG3C (supplemental Figs. 3*A* and 4*A*).

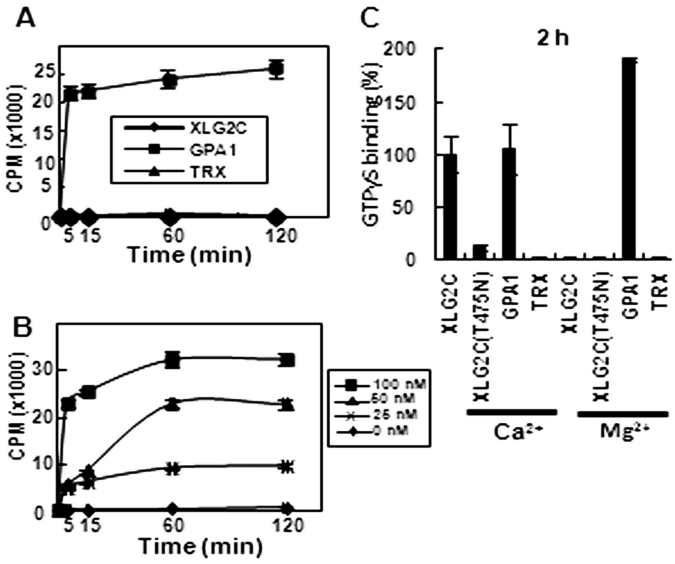

FIGURE 1. **XLG2 has GTP binding activity in the presence of Ca^{2+}.** *A*, time course of [^{35}S]GTPγS binding to GPA1 and lack of [^{35}S]GTPγS binding to XLG2C in the presence of $MgCl_2$. 100 nM XLG2C was incubated at 30 °C with 0.2 μM [^{35}S]GTPγS in the presence of 10 mM $MgCl_2$. 100 nM His_6 TRX and 100 nM His_6 TRX-tagged GPA1 were used as negative and positive controls, respectively. Aliquots (20 μl) were withdrawn at the indicated time points, filtered, and subjected to scintillation counting. *B*, time course of [^{35}S]GTPγS binding to XLG2 in the presence of different concentrations of Ca^{2+}. 100 nM XLG2C was incubated at 30 °C with 0.2 μM [^{35}S]GTPγS in the presence or absence of 10 mM $CaCl_2$. *C*, [^{35}S]GTPγS binding to XLG2C, its mutant form XLG2C(T475N), and GPA1 in the presence of $CaCl_2$ or $MgCl_2$. The amount of [^{35}S]GTPγS binding to XLG2C, XLG2C(T475N), and GPA1 was measured after a 2-h incubation in the presence of $CaCl_2$ or $MgCl_2$. *Error bars*, S.D.

Because heterotrimeric G protein α subunits, including *Arabidopsis* GPA1, have intrinsic GTPase activity, we examined the GTPase activity of XLG2C using thin layer chromatography (TLC) in the presence of various divalent cations. Although GPA1, like mammalian Gα subunits, exhibited the greatest hydrolytic activity in the presence of Mg^{2+}, XLG2C showed little or no GTPase activity under this condition (Fig. 2*A*). In contrast, XLG2C GTPase activity was observed in the presence of Ca^{2+} (Fig. 2, *A* and *B*), although this activity was less than that of GPA1 in the presence of Mg^{2+} (Fig. 2*A* and supplemental Fig. 2*C*). As expected, no GTPase activity was observed for the mutant form of XLG2C, XLG2C(T475N) (Fig. 2*B*). The GTPase activity of XLG2C protein, which has no tag, was similar to that of His_6 TRX-tagged XLG2C (supplemental Fig. 2*B*), indicating that His_6 TRX tag does not affect the GTP binding and GTPase activities of XLG C terminus proteins.

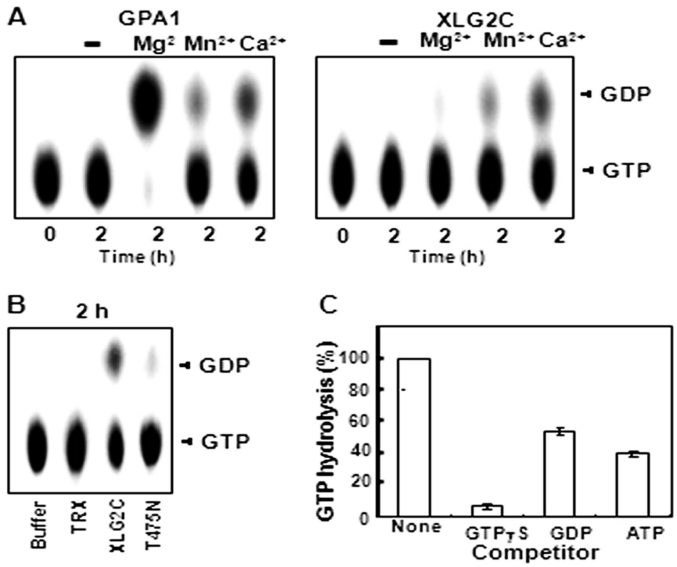

FIGURE 2. **XLG2 has GTPase activity in the presence of Ca^{2+}.** *A*, GTPase activity of GPA1 and XLG2C in the presence of different divalent cofactors. GTPase activity was measured using the PEI-cellulose TLC plate method. *B*, GTPase activity of XLG2 and lack of GTPase activity of XLG2C(T475N) in the presence of $CaCl_2$. The reactions were performed as described in *A*. Aliquots (2 μl) were withdrawn after incubation for 2 h and then separated by TLC. *C*, substrate competition test for XLG2 in the presence of $CaCl_2$. Reactions were performed as described in *A* in the presence of competitors (3 μM unlabeled GTPγS, GDP, or ATP). The graph was drawn using quantitative TLC results (supplemental Fig. 2*A*) measured by ImageJ software. GTP hydrolysis was calculated as GDP/(GTP + GDP). GTP hydrolysis in the absence of competitor was designated as 100%. *Error bars*, S.D.

TABLE 2

Comparison of GTPase activities of XLG proteins

GTPase activity calculated as the fraction of GTP remaining (GTP/(GTP + GDP)) after a 2-h incubation, as quantified by TLC. Smaller values indicate greater activity. Data shown are means ± S.D. of three independent replicates. ND, not determined. FL, full-length XLG proteins. C, C termini of XLG proteins, which include GTP binding domains.

	Mg^{2+}	Ca^{2+}
XLG1	ND	0.18 ± 0.05
XLG1C	0.8992 ± 0.08	0.36 ± 0.06
XLG2	ND	0.53 ± 0.11
XLG2C	0.9426 ± 0.03	0.68 ± 0.09
XLG3	ND	0.33 ± 0.06
XLG3C	0.9482 ± 0.0	0.46 ± 0.08

The specificity of the GTPase activity of XLG2C was also addressed (Fig. 2*C*). When a ~100-fold excess of cold GTPγS, GDP, or ATP was added to the reaction, GTPγS had the greatest competitive effect, indicating that XLG2C specifically binds GTP (Fig. 2*C*). The full-length XLG2 protein exhibited only slightly increased GTPase activity compared with XLG2 C terminus protein (Table 2 and supplemental Fig. 2*B*), suggesting that the N-terminal region of XLG2 is dispensable for the GTPase activity. Similar results were observed for XLG1 and XLG3 (Table 2 and supplemental Figs. 3 and 4).

RTV1 Is Identified as an XLG2-interacting Protein by Yeast Two-hybrid Screen—To address the functions of XLGs, we used a yeast two-hybrid screen to identify proteins that interact with XLG2. One XLG2-interacting protein recovered from the screen was RTV1 (related to vernalization 1) (At1g49480). *RTV1* encodes a predicted protein of 226 amino acids with a plant-specific B3 DNA binding domain and a nuclear localization signal (NLS) (56). RTV1 shows an overall 81% identity with

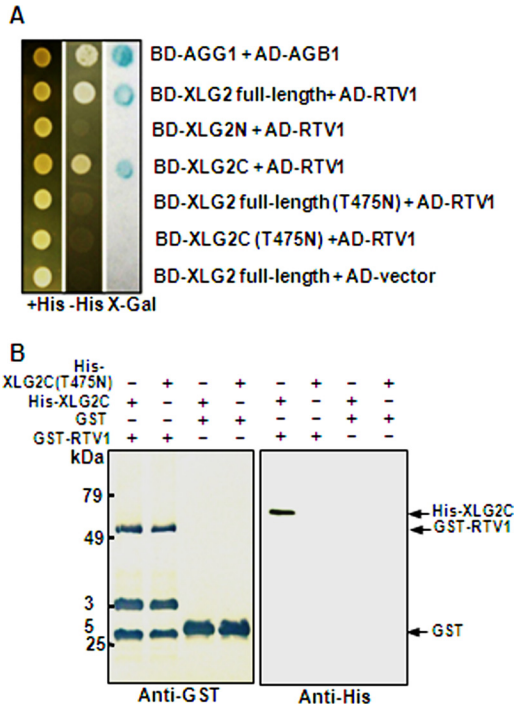

FIGURE 3. **XLG2 but not XLG2(T475N) interacts with RTV1.** *A*, yeast two-hybrid assay. β-Galactosidase activity was measured by the filter assay method (Invitrogen). The domains within XLG2 responsible for RTV1 binding were investigated. Wild type, domain deletion mutants, and a point mutant of *XLG2* (T475N) were fused to the bait (*BD*) vector, and a full-length cDNA of *RTV1* was fused to the prey (*AD*) vector. These constructs (described at the *right*) were co-transformed into pJG69-4A yeast cells, and their interactions were evaluated. AGG1 and AGB1 were used as a positive control for interaction (14). *B*, *in vitro* protein pull-down assay. Approximately 1 μg of GST or recombinant GST-tagged RTV1 was incubated with 1 μg of recombinant His-tagged AtXLG2C or AtXLG2C(T475N) and pulled down with GST resin after preblocking with 1% BSA. After five washes, the bound protein was fractionated by 12% SDS-PAGE and subjected to Western blot analysis with anti-GST or anti-His monoclonal antibodies. The extra bands may represent nonspecific cross-reactivity to bacterial proteins. Detection was by alkaline phosphatase/NBT directly on the blot membrane (*left*) or by enhanced chemiluminescence on x-ray film (*right*).

VRN1 in its amino acid sequence. VRN1 is a plant-specific B3-like DNA binding domain protein (57) that is required for maintenance of vernalization-mediated *FLC* repression and also promotes flowering in a vernalization-independent manner (58). To identify the domains of XLG2 that are responsible for RTV1 binding, we used partial cDNAs for additional yeast two-hybrid assays (Fig. 3*A*). Both full-length XLG2 and the C terminus of XLG2 interacted with RTV1, but the N terminus of XLG2 did not, indicating that the C terminus of XLG2 is responsible for the interaction in yeast.

Interestingly, the XLG2 mutant proteins, XLG2 full-length (T475N) and XLG2C(T475N), which do not bind GTP, did not show any interaction with RTV1 in yeast (Fig. 3*A*), suggesting that XLG2 interacts with RTV1 in a GTP-dependent manner. These results were further confirmed by *in vitro* pull-down assays using recombinant proteins. We found that His_6 TRX XLG2C but not His_6 TRX XLG2C(T475N) binds to GST-RTV1 *in vitro* (Fig. 3*B*). Thus, the GTP binding activity of XLG2 appears to be required for its interaction with RTV1. Given the sequence similarity between RTV1 and VRN1, we also tested whether VRN1 interacts with XLGs using the yeast two-hybrid assay. However, VRN1 did not interact with any of the three XLGs (data not shown).

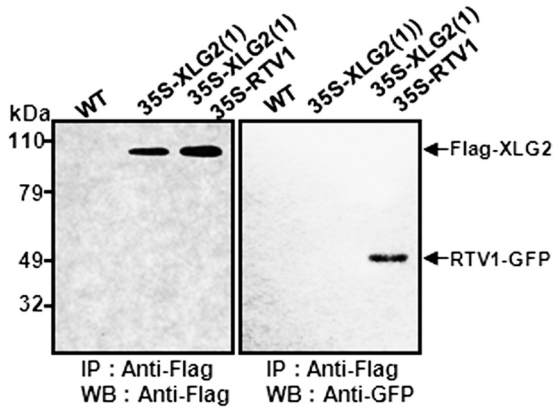

FIGURE 4. **XLG2 interacts with RTV1 *in planta*.** Co-immunoprecipitation analysis is shown. Total proteins were extracted from WT and *35S-FLAG-XLG2(1)* or *35S-FLAG-XLG2(1) 35S-RTV1-GFP* overexpression lines and then immunoprecipitated with anti-FLAG antibody. The immunoprecipitates were separated by 10% SDS-PAGE, transferred to polyvinylidene difluoride membranes, and blotted with anti-FLAG (*left*) or anti-GFP (*right*) antibody. *IP*, immunoprecipitation; *IB*, immunoblot.

XLG2 and RTV1 Interact in Vivo and RTV1 Protein Localizes to Nucleus—We used co-immunoprecipitation to test the protein-protein interaction between XLG2 and RTV1 *in vivo* (Fig. 4). Total proteins were extracted from wild type (non-transgenic), *35S-FLAG-XLG2(1)*, and *35S-FLAG-XLG2(1) 35S-RTV1-GFP* double-overexpressing lines. Protein extracts were immunoprecipitated with anti-FLAG antibody as probe, and then protein gel blotting was performed to detect RTV1-GFP with anti-GFP antibody (Fig. 4). RTV1-GFP was detected in the proteins from *35S::FLAG-XLG2(1) 35S-RTV1-GFP* double-overexpressing plants immunoprecipitated with anti-FLAG antibody. In control experiments, RTV1-GFP was not detected in the proteins immunoprecipitated with anti-FLAG antibody from WT or from *35S-FLAG-XLG2(1)* plants, confirming the physical interaction of XLG2 with RTV1 in plant cells.

Given that XLG2 and RTV1 interact *in planta*, they would be expected to show identical or overlapping subcellular localization. All XLG proteins, including XLG2, have a nuclear localization sequence and localize to the nucleus, as observed in transient expression assays (21). We carried out transient expression assays to ascertain the localization of RTV1, which also has a predicted nuclear localization sequence (RKKK; amino acids 69–72). The green fluorescence signal from RTV1-GFP overlaps with the red fluorescence from the RFP-tagged NLS peptide, indicating that RTV1 localizes to the nucleus (Fig. 5).

RTV1 Is Widely Expressed—We applied several complementary approaches to assess *RTV1* expression patterns. RT-PCR analysis showed that, similarly to *XLG2* (21), *RTV1* is expressed throughout the plant, including in roots, stems, leaves, flowers, and cauline leaves (Fig. 6*A*). We then used reporter gene analysis to examine expression patterns in more detail. Histochemical GUS staining of P_{RTV1}::*GUS* lines showed that *RTV1* is strongly expressed in cotyledon (*a*), shoot apical meristem (*b*), radicle (*c*), root tip (*d*), and staminar filaments (*e*) (Fig. 6*B*).

Given the sequence similarity between VRN1 and RTV1 and thus a possible role of *RTV1* in vernalization response, we also examined mRNA expression of *RTV1* during the course of ver-

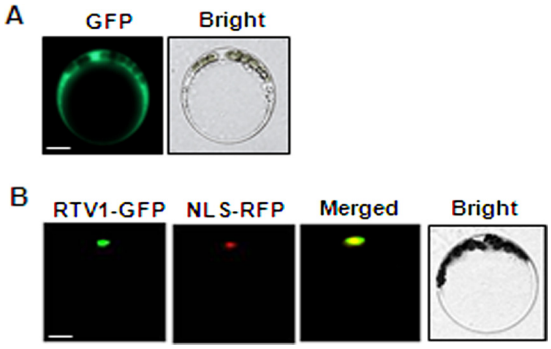

FIGURE 5. **RTV1 localizes to the nucleus.** *A*, *Arabidopsis* mesophyll protoplasts were transformed with GFP empty vector as a control. *Bar*, 10 μm. *B*, co-localization of RTV1-GFP with NLS-RFP (42). After co-transforming protoplasts with RTV1-GFP and NLS-RFP, the localization of these proteins was observed by fluorescence microscopy. *Yellow regions* in the *merged image* indicate overlap between the green and red fluorescent signals. *Bar*, 10 μm.

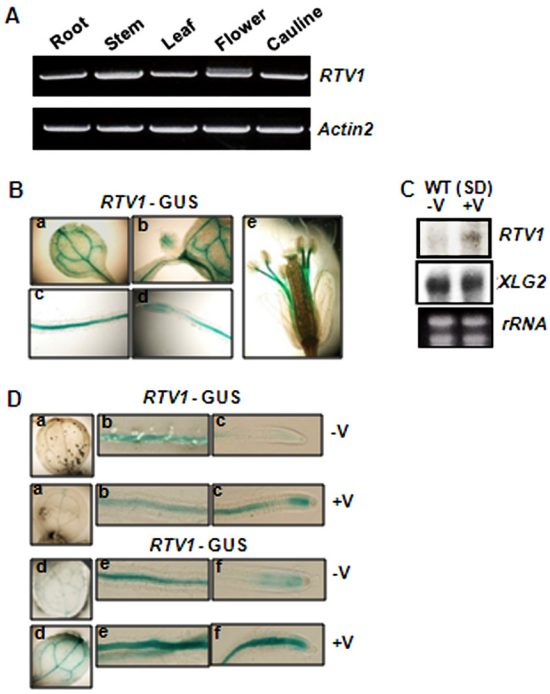

FIGURE 6. ***RTV1* is expressed ubiquitously and its expression is enhanced by vernalization treatment.** *A*, *RTV1* expression in various organs as determined by RT-PCR. *B*, histochemical GUS staining of transgenic *Arabidopsis* expressing an *RTV1* promoter-*GUS* fusion. *a*, cotyledon; *b*, shoot apical meristem; *c* and *d*, 7-day-old root; *e*, flower of 6-week-old plant. *a* and *d*, leaf; *b* and *e*, root; *c* and *f*, root tip. *C*, Northern blot analysis of *RTV1* and *XLG2* with (+*V*) or without (−*V*) 5 weeks of vernalization treatment. *D*, histochemical GUS staining of transgenic P_{RTV1}-*GUS* line with (+*V*) or without (−*V*) 5 weeks of cold treatment. For GUS staining, *a*–*c* and *d*–*f* were incubated for 3 and 6 h, respectively.

nalization treatment (Fig. 6, *C* and *D*, and supplemental Fig. 5). RNA blot analysis showed that mRNA expression of *RTV1*, but not of *XLG2*, is increased after a 5-week cold treatment (Fig. 6*C*). Up-regulation of *RTV1* by a 5-week cold treatment was also observed using P_{RTV1}-*GUS* (Fig. 6*D*). Stronger expression of P_{RTV1}-*GUS* was observed in plants that experienced a long term cold treatment (Fig. 6*D*, +*V*) compared with a control without cold treatment (Fig. 6*D*, −*V*).

To further dissect the increased level of *RTV1* mRNA, we performed quantitative real-time RT-PCR using samples subjected to cold treatments ranging from 1 h to 5 weeks

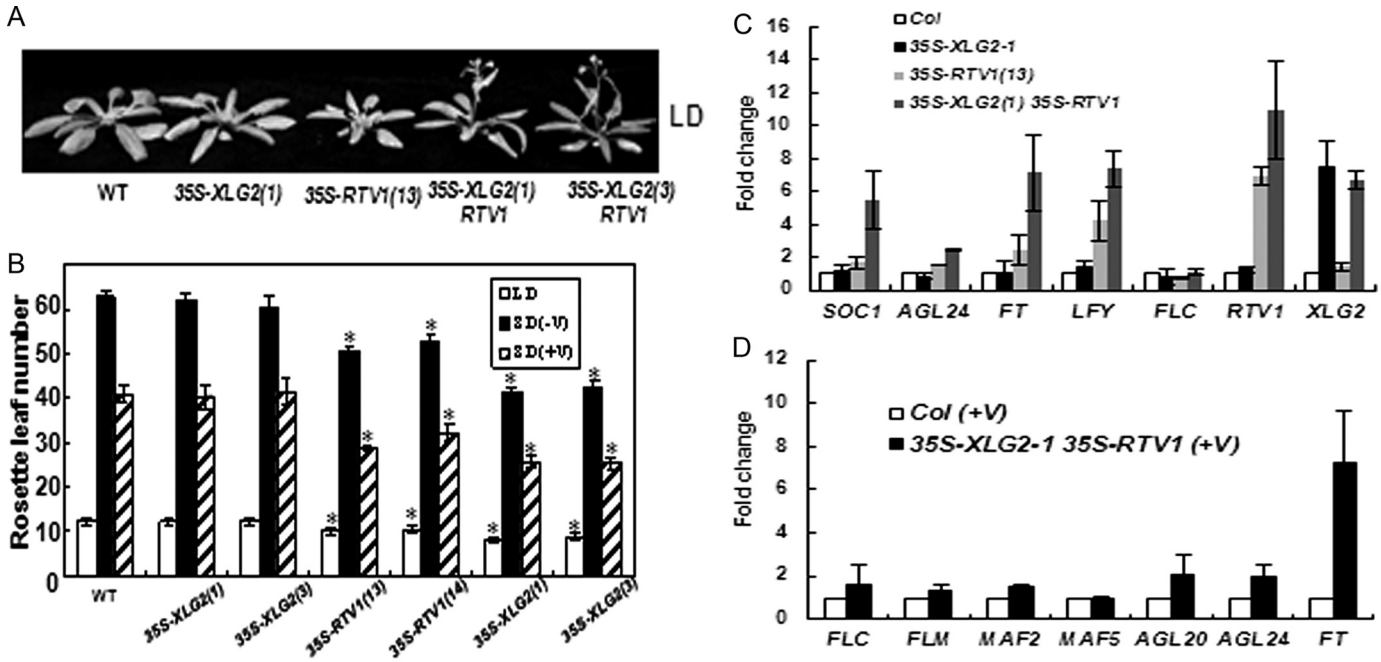

FIGURE 7. ***35S-FLAG-RTV1* plants flower early in both LD and SD, and earlier flowering is further enhanced in *35S-FLAG-XLG2 35S-RTV1-GFP* plants.** *A*, early flowering of *35S-FLAG-XLG2 35S-RTV1-GFP* in LD. *B*, flowering times were determined as total rosette leaf number at the time of flowering under LD and SD conditions with (+*V*) or without (−*V*) 5 weeks of cold treatment. At least 12 plants of each genotype were used. Statistical significance was determined by Student's *t* test (*, $p < 0.001$ *versus* Col). *C*, all transcript levels were normalized to *ACTIN2* levels using the formula, $C_T = C_T$(each gene) − C_T(*ACTIN2*). -Fold changes are relative to results from wild type (*Col*). Real-time RT-PCR was performed with cDNAs from 2-week-old wild type and transgenic plants grown in SD conditions. Each *bar* represents an average of three independent replicate experiments. *D*, the expression of *FLC*, *FLC* clade (*MAFs*), and floral integrator genes in *35S-FLAG-XLG2 35S-RTV1-GFP* plants after 5 weeks of cold treatment (+*V*). All results were obtained as described in *C*.

(supplemental Fig. 5). The mRNA level of *RTV1* was rapidly increased almost 10-fold within 1 h of cold treatment and then decreased below the level of no cold treatment after 3 h of cold treatment. *RTV1* mRNA expression eventually increased again ~2-fold after a 5-week cold treatment (supplemental Fig. 5). *XLG2* mRNA also exhibited the rapid increase within 1 h of cold treatment and the decrease after 3 h of cold treatment. Unlike *RTV1*, however, the level of *XLG2* mRNA remained unchanged after a 5-week cold treatment (Fig. 6*C* and supplemental Fig. 5).

RTV1 Overexpression Promotes Early Flowering, Which Is Enhanced by Co-overexpression of XLG2—The ectopic expression of *VRN1* causes early flowering due to the activation of *FT* and *SOC1* (58). We accordingly examined flowering times of transgenic plants overexpressing *RTV1*. The *35S-FLAG-RTV1* plants exhibited rapid flowering under SD and a slight acceleration of flowering under LD (Fig. 7, *A* and *B*). In addition, when *35S-FLAG-RTV1* plants were vernalized, flowering was further accelerated (Fig. 7, *A* and *B*). Because XLG2 and RTV1 interact, we also evaluated the flowering time of *35S-FLAG-XLG2 35S-RTV1-GFP* double overexpression lines. Interestingly, double overexpressor (Fig. 7, *A* and *B*, *35S-FLAG-XLG2 35S-RTV1-GFP*) plants showed earlier flowering under LD and SD compared with both WT and *35S-FLAG-RTV1* plants, with or without vernalization treatment (Fig. 7*B*). Thus, the interaction between XLG2 and RTV1 appears to enhance RTV1 activity *in vivo*. To investigate the molecular basis of this early flowering phenotype, we examined the expression of floral pathway genes in *35S-FLAG-XLG2* and *35S-FLAG-RTV1* overexpression lines and in *35S-FLAG-XLG2 35S-RTV1-GFP* double overexpression lines under SD using quantitative RT-PCR. Introduction of *35S-FLAG-XLG2* alone did not promote transcript levels of the floral pathway genes *SOC1*, *AGL24*, *FT*, and *LFY* (Fig. 7*C*). However, the abundance of these transcripts was increased in *35S-FLAG-RTV1* plants and even more so in *35S-FLAG-XLG2 35S-RTV1-GFP* plants (Fig. 7*C*).

Vernalization triggers the repression of *FLC* and other *FLC* clade genes (37, 59). mRNA levels of *FLC* and its clade genes *MAF1*, *MAF2*, and *MAF5* in *35S-FLAG-RTV1* and *35S-FLAG-XLG2 35S-RTV1-GFP* plants immediately after vernalization showed no significant difference compared with vernalized wild type in the extent of this repression (*i.e.* -fold change compared with Col was <2). After vernalization, however, the floral pathway integrator genes *SOC1* and *AGL24* and particularly the levels of *FT* mRNA were higher in these lines than in Col (*i.e.* -fold change compared with Col was >2) (Fig. 7*D*). To analyze the effect of *ft* mutation (60) on the flowering time of *35S-RTV1-GFP* plants, *35S-RTV1-GFP* construct was transformed into the *ft* mutant, and flowering times were determined (Fig. 8). *35S-RTV1-GFP* in the *ft* mutant background had the same late flowering phenotype as *ft* mutants (Fig. 8), indicating that early flowering of *35S*::*RTV1* requires the elevated expression of *FT*. Therefore, accelerated flowering of overexpressing *XLG2* and *RTV1* plants (with or without vernalization) apparently occurs directly through regulation of the floral pathway integrator gene, *FT*, through a mechanism independent of repression of *FLC* and its clade genes.

RTV1 Binds DNA and XLG2 Enhances This DNA Binding Activity—VRN1 shows a non-sequence-specific DNA binding activity *in vitro* (58). Given the sequence similarity between

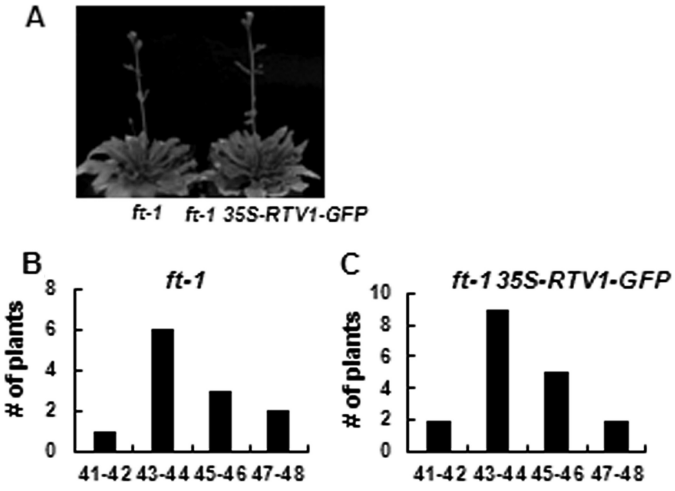

FIGURE 8. **Flowering phenotypes of *35S-RTV1 ft-1*.** *A*, *35S-RTV1 ft-1* flowering is similar to *ft-1*. *B* and *C*, data represent plant frequency distributions based on rosette leaf number at flowering under LD *ft-1* ($n = 12$) (*B*) and *35S-RTV1 ft-1* ($n = 18$ T1 individuals) (*C*). *Error bars*, S.D.

VRN1 and RTV1 and the nuclear localization of RTV1, we examined the DNA binding activity of recombinant RTV1 protein. EMSAs were performed using DNA fragments derived from promoters of *FLC*, *SOC1*, *FT*, *VRN2*, or *DFR* (dihydroflavonol 4-reductase). Recombinant RTV1 protein bound to all DNA fragments tested (Fig. 9*A* and supplemental Fig. 6). These DNA fragments do not share any common sequence motif, illustrating that, similar to VRN1, RTV1 has non-sequence-specific DNA binding activity, at least in these *in vitro* assays. The interaction between XLG2 and RTV1 prompted us to hypothesize that this interaction may modulate the DNA binding activity of RTV1. Accordingly, recombinant XLG2 C-terminal domain protein (XLG2C), which contains the RTV1 interaction domains (Fig. 3), was added in the reaction with RTV1, and the binding strength was evaluated by the amount of probe retardation (Fig. 9*B*). The addition of XLG2C increased the DNA binding activity of RTV1 (Fig. 9*B*), whereas the mutant protein XLG2C(T475N), which fails to interact with RTV1, did not (Fig. 8*B*). Because XLG2C(T475N) mutant protein also fails to bind GTP *in vitro* (Fig. 1*C*), we examined the effect of GTP binding of XLG2C on the DNA binding activity of RTV1. XLG2C, GTPγS, and Ca^{2+} were added in the reaction together with RTV1. Under these conditions, XLG2C formed a super-complex with RTV1 and probes, suggesting that activation of XLG2C by GTP binding contributes to the enhanced DNA binding of RTV1 *in vitro* (Fig. 9*C*).

RTV1 Is Associated with FT and SOC1 Promoters in Vivo—We showed that *RTV1* overexpression lines show early flowering due to increased expression of floral pathway integrator genes independent of regulation of *FLC* expression (Figs. 7 and 8) and that RTV1 binds to DNA in a non-sequence-specific manner *in vitro* (Fig. 9*A* and supplemental Fig. 9). To address whether RTV1 binds to promoters of floral pathway integrator genes, such as *FT* and *SOC1*, *in vivo*, ChIP assays were employed. For these assays, wild type, *35S-FLAG-RTV1(13)*, and *35S-FLAG-XLG2(1) 35S-RTV1-GFP* double-overexpresssing lines were used. After immunoprecipitation with anti-FLAG or anti-GFP antibodies, enrichment of *FT* and *SOC1* promoter regions was assayed by quantitative PCR. As shown in Fig. 10, *B* and *C*, enrichment of the *FT* promoter region, 1–200 bp upstream from the start codon (P1) was observed in the *35S-FLAG-RTV1(13)* line, with slightly enhanced enrichment in the *35S-FLAG-XLG2(1) 35S-RTV1-GFP* overexpression lines. In addition, *SOC1* promoter regions were not enriched in *35S-FLAG-RTV1(13)*, whereas enrichment of the *SOC1* promoter region, 1–200 bp upstream from the start codon (P1) was observed from the *35S-FLAG-XLG2(1) 35S-RTV1-GFP* (Fig. 10*C*). No enrichment of *FLC* regions was observed in either the *35S-FLAG-RTV1(13)* line or the *35S-FLAG-XLG2(1) 35S-RTV1-GFP* line (Fig. 10, *B* and *C*). Taken together, our results indicate that XLG2 promotes the DNA binding activity of RTV1 specifically to promoter regions of *FT* and *SOC1 in vivo* and thus leads to the activation of floral integrator genes (Fig. 11).

DISCUSSION

XLG Proteins Are Specific GTPases—Here we report new biochemical and functional properties of the XLG proteins. Conventional Gα proteins have highly conserved domains involved in GTP binding and hydrolysis. Because of variations in amino acid sequences within these domains in the three XLG proteins (Table 1), it was not clear whether or not the XLG proteins function as GTPases. XLG1 had been shown previously to bind GTP (20), but GTP binding of XLG2 and XLG3, or GTPase activity of any of the XLG proteins had not been evaluated. In this study, we show that the three XLG proteins indeed specifically bind GTP and possess GTPase activity. Thus, we provide biochemical evidence that the XLG proteins, despite their unusual structure, are *bona fide* G proteins. Given the variations in amino acid sequences of the XLG GTP-binding domains, we initially hypothesized that the XLG-specific N termini might provide structural scaffolds that enable GTP binding. However, this appears not to be the case because the C termini of the XLGs alone are sufficient for GTP binding and GTPase activity (Fig. 1 and supplemental Figs. 2–4). The specific functions of the unique N termini of the XLG proteins remain to be uncovered. XLG2, which is the most divergent of the three XLGs in the G-1, G-2, G-3, and G-4 domains, also has the slowest GTPase activity (Table 2). Other types of G proteins, such as Ras and EF-Tu (61), associate with GTPase-activating proteins (GAPs) (62). It will be interesting in the future to determine whether GAPs exist for the XLGs.

The XLGs are distinct from canonical Gα subunits in their dependence on Ca^{2+}, rather than Mg^{2+}, as a cofactor. The G-1 to G-3 domains of G proteins provide critical contacts for the α-, β-, and γ-phosphates of the guanine nucleotide and also for the coordination of Mg^{2+} (50). The G-4 and G-5 domains are important for the binding of the guanine ring (50). XLG2 has the conserved amino acid motifs in the G-1, G-2, and G-4 regions. XLG2 utilizes Ca^{2+} but not Mg^{2+} as a cofactor although it has the well conserved threonine residue in the G-2 region (Table 1), which plays a critical role in coordinating Mg^{2+} (50). However, XLG proteins do not have the conserved motifs of the G-3 and G-5 regions (21) (Table 1). The glutamine residue in the G-3 (D*XX*GQ) domain is involved in coordination of Mg^{2+} mediated by water, and the main chain of the

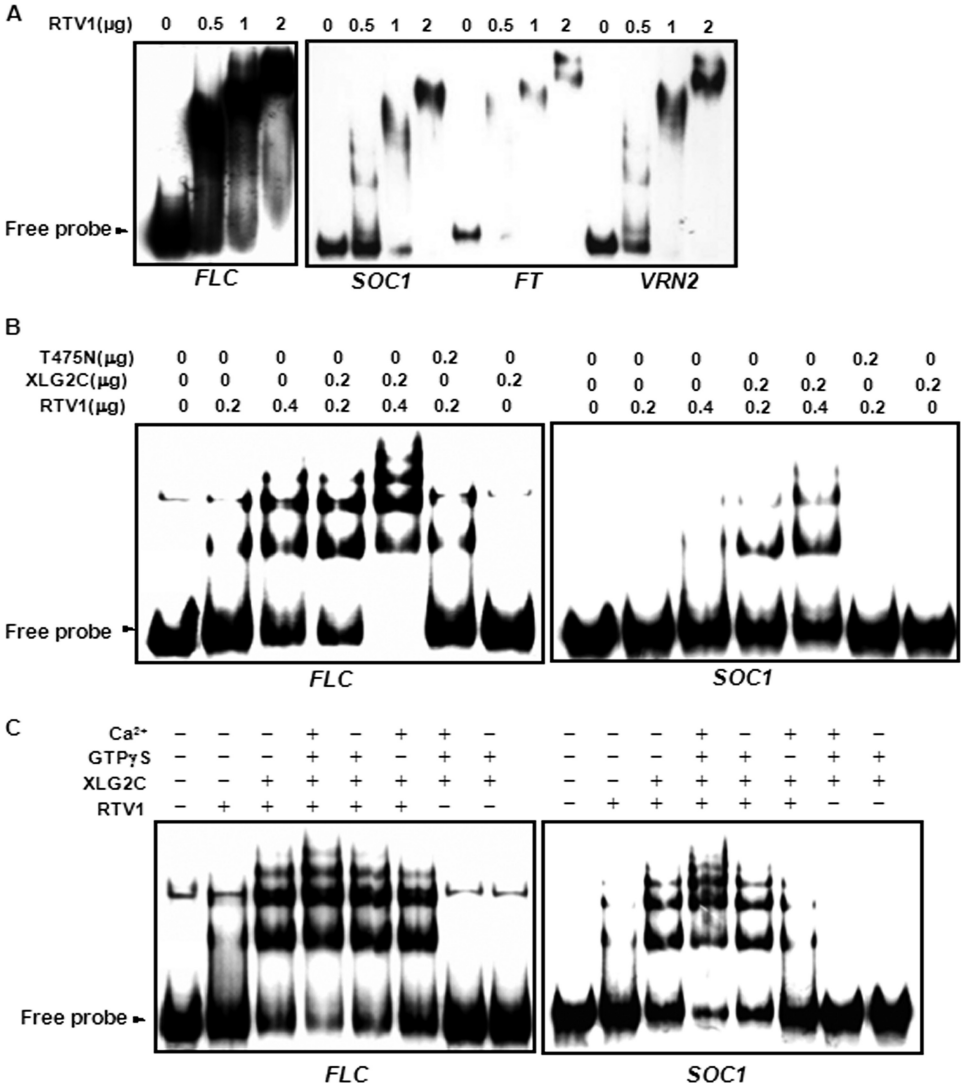

FIGURE 9. **RTV1 has non-sequence-specific DNA binding activity *in vitro* that is enhanced by XLG2.** *A*, EMSA of RTV1 using *FLC*, *SOC1*, *FT*, or *VRN2* promoter regions. RTV1 protein (0–57 nM; 0–2 μg) and 400-bp radiolabeled double-stranded *FLC*, *SOC1*, *FT*, or *VRN2* probe were incubated and then separated on a 5% Tris-borate EDTA-polyacrylamide gel. *B*, increased DNA binding by RTV1 in the presence of XLG2C but not in the presence of XLG2C(T475N). The reaction was performed as described in *A* together with 50 nM XLG2C or XLG2C(T475N) using *FLC* or *SOC1* probes, respectively. *C*, the effect of GTPγS binding by XLG2 in the presence of Ca^{2+}. The reaction was performed as described in *B* together with 1 mM GTPγS and 10 mM Ca^{2+} using *FLC* or *SOC1* probes, respectively.

glycine residue forms hydrogen bonds with the γ-phosphate of GTP (49, 51). When introduced in Ras, virtually all mutations in the G-3 domain reduce its GTPase activity and disrupt Ras binding to Ras-GAP (63). Corresponding mutations in $G\alpha_s$ (64, 65) and in $G\alpha_{i1}$ (66) also reduce the GTPase activity. In addition, mutation at the G-5 (TCA) alanine in $G\alpha_i$ promotes rapid GDP dissociation, although the intrinsic GTPase activity of $G\alpha_i$ is not changed (67). Taken together, variations in amino acid sequences of XLG2 and the other two XLG proteins probably contribute to their different cofactor requirement.

In summary, our data demonstrate that all three XLG proteins exhibit both GTP binding and GTPase activity. Our results also revealed an interesting divergence from Gα proteins because XLG proteins cannot utilize Mg^{2+} as a cofactor. The unusual requirement for Ca^{2+} in XLG protein GTP binding and hydrolysis raises the possibility that XLG proteins may be involved in the regulation of a variety of physiological and metabolic processes that are dependent on internal Ca^{2+} concentration, a well known component in many signal transduction chains in plants and other eukaryotes (68).

RTV1 Is an XLG2-interacting Protein—RTV1 was identified as an XLG2-interacting protein by a yeast two-hybrid screen using XLG2 as bait (Fig. 3*A*). We confirmed the interaction between RTV1 and XLG2 *in vitro* and *in planta* (Fig. 3*B* and Fig. 4), indicating that RTV1 is a *bona fide* interacting protein of XLG2. Interestingly, the Gα-like C terminus of XLG2, rather than the N terminus, interacts with RTV1 (Fig. 3*A*). The interaction is not observed with the XLG2C(T475N) mutant (Fig. 3, *A* and *B*), which lacks GTP binding activity (Fig. 1*C*). This suggests that GTP binding by XLG2 plays an important role in protein-protein interaction.

The *RTV1* gene encodes a protein with a B3-like DNA binding domain, a domain that is unique to plants (56). The expression of *RTV1* in vasculature is similar to that of other floral regulators, such as *FT* (69, 70), establishing an overlapping expression profile between RTV1 and the RTV1 target, *FT*, and

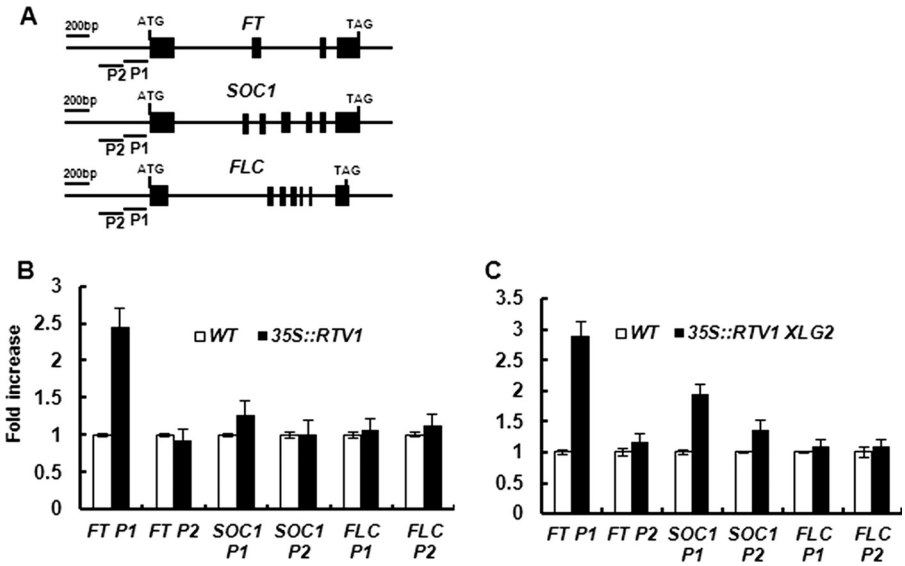

FIGURE 10. **RTV1 is associated with *FT* and *SOC1* chromatin at their promoter regions.** *A*, schematic diagram of the *FT*, *SOC1*, and *FLC* genomic regions. Exons are represented by *black boxes*, whereas introns and upstream regions are represented by *black lines*. Primer regions used in ChIP assays are designated as P1 and P2. *B* and *C*, ChIP-quantitative PCR analyses. WT, *35S-FLAG-RTV1(13)* (*B*), and *35S-FLAG-XLG2(1) 35S-RTV1-GFP* (*C*) transgenic seedlings were grown under SD. Chromatin was isolated with extraction buffers. Anti-FLAG or anti-GFP antibodies were used for immunoprecipitation. Precipitated chromatin from ChIP assays from WT and transgenic seedlings was quantified by quantitative PCR with specific primers for regions indicated in *A*. *Error bars*, S.D.

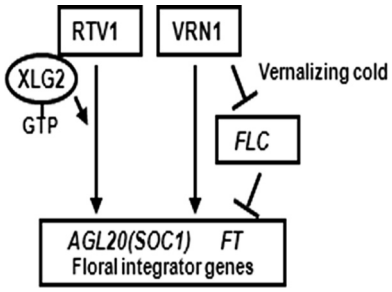

FIGURE 11. **Model for the roles of *RTV1* and *XLG2* in the regulation of floral integrator genes in *Arabidopsis*.** The GTP-bound form of XLG2 promotes RTV1 DNA binding to floral integrator genes, *FT* and *SOC1*, leading to early flowering.

suggesting that RTV1 is capable of regulating *FT* in locations where *FT* is expressed. The expression pattern of *RTV1* and the nuclear localization of RTV1 are also very similar to those of XLG2 (Fig. 5 and 6) (21), consistent with *in planta* interaction of the proteins.

RTV1 Promotes Floral Integrator Gene Expression and Flowering via an XLG2-related Mechanism—Overexpression of *RTV1* led to early flowering (Fig. 7) through increased expression of floral integrator genes, such as *FT* and *SOC1* (Fig. 7*C*). Consistent with this model, introgression of 35S::RTV1 into an *ft* background eliminated the early flowering phenotype (Fig. 8). Moreover, when *RTV1* was overexpressed together with *XLG2*, the expression of the floral integrator genes was further enhanced, and these plants showed even earlier flowering compared with *RTV1*-only-overexpressing lines (Fig. 7). These results lead to a model whereby XLG2 interaction with RTV1 promotes RTV1 activity, leading to enhanced expression of the floral pathway integrator genes (Fig. 11).

XLG2 Promotes RTV1 Binding to Promoter Regions of Floral Integrator Genes—RTV1 exhibits strong DNA binding activities *in vitro* with DNA fragments derived from promoter regions of *FLC*, *SOC1*, *FT*, and *VRN2* (Fig. 9) as well as with the promoter of the non-flowering related gene *DRF* (supplemental Fig. 6). Such non-sequence-specific binding to DNA fragments *in vitro* was also observed for VRN1, which also belongs to the B3 domain superfamily (58).

Swaminathan *et al.* (56) classified *B3* genes into four families that are typified by *ABI3* (abscisic acid-insensitive 3 (71)), *ARF1* (auxin-responsive factor 1 (72)), *RAV1* (related to ABI3/VP1 (73)), and *REM* (reproductive meristem). The 76 *REM* genes in *Arabidopsis* have been divided into six subgroups (A–F) based on phylogenetic analysis (56). *RTV1* and *VRN1* belong to the six genes of subgroup A of the *REM* family. *VRN1* has been the only *REM* gene with known function (58). Unlike other B3 domain proteins, which show sequence-specific DNA binding (*e.g.* ABI3, RAV1, and auxin-response factors), both VRN1 and RTV1 bind to DNA in a non-sequence-specific manner *in vitro* (58). It is interesting to note that XLG2C enhances the DNA binding activity of RTV1 (Fig. 9, *B* and *C*). XLG2 in the presence of Ca^{2+} and GTPγS enhances the DNA binding activity of RTV1 even further (Fig. 9*C*), whereas the T475N mutant of XLG2C, which does not bind GTP, has no effect on the DNA binding activity of RTV1 (Fig. 9*B*). Taken together, these results suggest that XLG2 activation caused by GTP binding in the presence of Ca^{2+} enhances the DNA binding activity of RTV1.

Although we did not observe sequence-specific DNA binding of RTV1 *in vitro*, specificity may be conferred by other components, such as other interacting proteins, present *in planta* but not *in vitro*. In fact, our ChIP analyses showed that RTV1 binds only to certain target genes *in planta*. In ChIP assays using 10-day-old *35S-FLAG-RTV1(13)* and *35S-FLAG-XLG2(1) 35S-RTV1-GFP* seedlings, we consistently found that RTV1 directly interacts with *FT* and *SOC1* promoters. Moreover, a slight increase of RTV1 at the *FT* promoter and an enrichment of RTV1 at the *SOC1* promoter were observed in *35S-FLAG-XLG2(1) 35S-RTV1-GFP* seedlings compared with *35S-FLAG-RTV1(13)* (Fig. 10, *B* and *C*). This suggests that

XLG2 facilitates RTV1 activation, which then results in transcriptional activation of *FT* and *SOC1*, an interpretation that is also consistent with our *in vitro* gel shift assays (Fig. 9*C*) and our gene expression assays (Fig. 7).

We did not observe any significant enrichment of RTV1 at *FLC* regions by ChIP assays (Fig. 10, *B* and *C*); nor did we observe any enhanced repression of FLC upon vernalization of *35S-FLAG-XLG2(1) 35S-RTV1-GFP* lines (Fig. 7*D*). This suggests that *RTV1* and *XLG2* overexpression directly activate floral integrator genes in an FLC-independent manner. VRN1, which shares significant sequence homology with RTV1, also activates floral integrator genes via an FLC-independent pathway (58), and ectopic expression of RTV1 also accelerates flowering. These two proteins differ, however, in that VRN1, but not RTV1, has an additional function in stabilizing FLC repression postvernalization (58), and RTV1, but not VRN1, binds and is regulated by XLG2 (Fig. 11).

In summary, our work provides new insight into signaling by Ca^{2+} and G proteins. We show that RTV1 and XLG2 function together in the regulation of flowering time. *FT* and *SOC1* are direct targets of RTV1. It is likely that GTP-bound XLG2 and/or XLG2 cycling between GTP- and GDP-bound states, which occur in the presence of Ca^{2+}, are required for enhanced RTV1 association with targets such as FT and SOC1. Circadian oscillations in intracellular free calcium ions ($[Ca^{2+}]_i$) occur and encode photoperiodic information (74, 75). It is interesting to note that *XLG2* and *RTV1* transcripts exhibit in-phase circadian oscillation (see the Diurnal Search Tool Web site). It is tantalizing to speculate that XLG2-RTV1 mediates some of the outputs from the oscillations in $[Ca^{2+}]_i$. However, the role of $[Ca^{2+}]_i$ oscillation in flowering time control is poorly understood. Further studies on the regulatory network of Ca^{2+}, XLG2, and RTV1 should provide interesting insights into the roles of XLG proteins in Ca^{2+}-mediated signaling pathways.

REFERENCES

1. Hepler, J. R., and Gilman, A. G. (1992) G proteins. *Trends Biochem. Sci.* **17,** 383–387
2. Assmann, S. M. (2002) Heterotrimeric and unconventional GTP binding proteins in plant cell signaling. *Plant Cell* **14,** S355–S373
3. Jones, A. M., and Assmann, S. M. (2004) Plants: the latest model system for 6-protein research. *EMBO Rep.* **5,** S572–S578
4. Ma, H. (1994) GTP-binding proteins in plants. New members of an old family. *Plant Mol. Biol.* **26,** 1611–1636
5. Gilman, A. G. (1987) G proteins. Transducers of receptor-generated signals. *Annu. Rev. Biochem.* **56,** 615–649
6. Gutkind, J. S. (1998) The pathways connecting G protein-coupled receptors to the nucleus through divergent mitogen-activated protein kinase cascades. *J. Biol. Chem.* **273,** 1839–1842
7. Hamm, H. E. (1998) The many faces of G protein signaling. *J. Biol. Chem.* **273,** 669–672
8. McCudden, C. R., Hains, M. D., Kimple, R. J., Siderovski, D. P., and Willard, F. S. (2005) G-protein signaling. Back to the future. *Cell Mol. Life Sci.* **62,** 551–577
9. Assmann, S. M. (2004) Plant G proteins, phytohormones, and plasticity. Three questions and a speculation. *Sci. STKE* **2004,** re20
10. Temple, B. R., and Jones, A. M. (2007) The plant heterotrimeric G-protein complex. *Annu. Rev. Plant Biol.* **58,** 249–266
11. Assmann, S. M. (2005) G proteins Go green. A plant G protein signaling FAQ sheet. *Science* **310,** 71–73
12. Ma, H., Yanofsky, M. F., and Meyerowitz, E. M. (1990) Molecular cloning and characterization of GPA1, a G protein α subunit gene from *Arabidopsis thaliana*. *Proc. Natl. Acad. Sci. U.S.A.* **87,** 3821–3825
13. Weiss, C. A., Garnaat, C. W., Mukai, K., Hu, Y., and Ma, H. (1994) Isolation of cDNAs encoding guanine nucleotide-binding protein β-subunit homologues from maize (ZGB1) and *Arabidopsis* (AGB1). *Proc. Natl. Acad. Sci. U.S.A.* **91,** 9554–9558
14. Mason, M. G., and Botella, J. R. (2000) Completing the heterotrimer. Isolation and characterization of an *Arabidopsis thaliana* G protein γ-subunit cDNA. *Proc. Natl. Acad. Sci. U.S.A.* **97,** 14784–14788
15. Mason, M. G., and Botella, J. R. (2001) Isolation of a novel G-protein γ-subunit from *Arabidopsis thaliana* and its interaction with Gβ. *Biochim. Biophys. Acta* **1520,** 147–153
16. Gookin, T. E., Kim, J., and Assmann, S. M. (2008) Whole proteome identification of plant candidate G-protein coupled receptors in *Arabidopsis*, rice, and poplar. Computational prediction and *in vivo* protein coupling. *Genome Biol.* **9,** R120
17. Moriyama, E. N., Strope, P. K., Opiyo, S. O., Chen, Z., and Jones, A. M. (2006) Mining the *Arabidopsis thaliana* genome for highly divergent seven-transmembrane receptors. *Genome Biol.* **7,** R96
18. Chakravorty, D., Trusov, Y., Zhang, W., Acharya, B. R., Sheahan, M. B., McCurdy, D. W., Assmann, S. M., and Botella, J. R. (2011) An atypical heterotrimeric G-protein γ-subunit is involved in guard cell K^+-channel regulation and morphological development in *Arabidopsis thaliana*. *Plant J.* **67,** 840–851
19. Perfus-Barbeoch, L., Jones, A. M., and Assmann, S. M. (2004) Plant heterotrimeric G protein function. Insights from *Arabidopsis* and rice mutants. *Curr. Opin. Plant Biol.* **7,** 719–731
20. Lee, Y. R., and Assmann, S. M. (1999) *Arabidopsis thaliana* "extra-large GTP-binding protein" (AtXLG1). A new class of G-protein. *Plant Mol. Biol.* **40,** 55–64
21. Ding, L., Pandey, S., and Assmann, S. M. (2008) *Arabidopsis* extra-large G proteins (XLGs) regulate root morphogenesis. *Plant J.* **53,** 248–263
22. Pandey, S., Monshausen, G. B., Ding, L., and Assmann, S. M. (2008) Regulation of root-wave response by extra large and conventional G proteins in *Arabidopsis thaliana*. *Plant J.* **55,** 311–322
23. Zhu, H., Li, G. J., Ding, L., Cui, X., Berg, H., Assmann, S. M., and Xia, Y. (2009) *Arabidopsis* extra large G-protein 2 (XLG2) interacts with the Gβ subunit of heterotrimeric G protein and functions in disease resistance. *Mol. Plant* **2,** 513–525
24. Parcy, F. (2005) Flowering. A time for integration. *Int. J. Dev. Biol.* **49,** 585–593
25. Moon, J., Lee, H., Kim, M., and Lee, I. (2005) Analysis of flowering pathway integrators in *Arabidopsis*. *Plant Cell Physiol.* **46,** 292–299
26. Michael, T. P., Salomé, P. A., Yu, H. J., Spencer, T. R., Sharp, E. L., McPeek, M. A., Alonso, J. M., Ecker, J. R., and McClung, C. R. (2003) Enhanced fitness conferred by naturally occurring variation in the circadian clock. *Science* **302,** 1049–1053
27. Liu, C., Chen, H., Er, H. L., Soo, H. M., Kumar, P. P., Han, J. H., Liou, Y. C., and Yu, H. (2008) Direct interaction of AGL24 and SOC1 integrates flowering signals in *Arabidopsis*. *Development* **135,** 1481–1491
28. Zeevaart, J. A. (2008) Leaf-produced floral signals. *Curr. Opin. Plant Biol.* **11,** 541–547
29. Turck, F., Fornara, F., and Coupland, G. (2008) Regulation and identity of florigen. FLOWERING LOCUS T moves center stage. *Annu. Rev. Plant Biol.* **59,** 573–594
30. Abe, M., Kobayashi, Y., Yamamoto, S., Daimon, Y., Yamaguchi, A., Ikeda, Y., Ichinoki, H., Notaguchi, M., Goto, K., and Araki, T. (2005) FD, a bZIP protein mediating signals from the floral pathway integrator FT at the shoot apex. *Science* **309,** 1052–1056
31. Melzer, S., Lens, F., Gennen, J., Vanneste, S., Rohde, A., and Beeckman, T. (2008) Flowering-time genes modulate meristem determinacy and growth form in *Arabidopsis thaliana*. *Nat. Genet.* **40,** 1489–1492
32. Samach, A., Onouchi, H., Gold, S. E., Ditta, G. S., Schwarz-Sommer, Z., Yanofsky, M. F., and Coupland, G. (2000) Distinct roles of CONSTANS target genes in reproductive development of *Arabidopsis*. *Science* **288,** 1613–1616
33. Hepworth, S. R., Valverde, F., Ravenscroft, D., Mouradov, A., and Coupland, G. (2002) Antagonistic regulation of flowering-time gene SOC1 by CONSTANS and FLC via separate promoter motifs. *EMBO J.* **21,**

4327–4337
34. Sung, S., and Amasino, R. M. (2004) Vernalization in *Arabidopsis thaliana* is mediated by the PHD finger protein VIN3. *Nature* **427,** 159–164
35. Michaels, S. D., and Amasino, R. M. (2001) Loss of FLOWERING LOCUS C activity eliminates the late-flowering phenotype of FRIGIDA and autonomous pathway mutations but not responsiveness to vernalization. *Plant Cell* **13,** 935–941
36. Bastow, R., Mylne, J. S., Lister, C., Lippman, Z., Martienssen, R. A., and Dean, C. (2004) Vernalization requires epigenetic silencing of FLC by histone methylation. *Nature* **427,** 164–167
37. Sung, S., He, Y., Eshoo, T. W., Tamada, Y., Johnson, L., Nakahigashi, K., Goto, K., Jacobsen, S. E., and Amasino, R. M. (2006) Epigenetic maintenance of the vernalized state in *Arabidopsis thaliana* requires LIKE HETEROCHROMATIN PROTEIN 1. *Nat. Genet.* **38,** 706–710
38. Northup, J. K., Smigel, M. D., and Gilman, A. G. (1982) The guanine nucleotide activating site of the regulatory component of adenylate cyclase. Identification by ligand binding. *J. Biol. Chem.* **257,** 11416–11423
39. Smigel, M. D., Northup, J. K., and Gilman, A. G. (1982) Characteristics of the guanine nucleotide-binding regulatory component of adenylate cyclase. *Recent Prog. Horm. Res.* **38,** 601–624
40. Heo, J. B., Rho, H. S., Kim, S. W., Hwang, S. M., Kwon, H. J., Nahm, M. Y., Bang, W. Y., and Bahk, J. D. (2005) OsGAP1 functions as a positive regulator of OsRab11-mediated TGN to PM or vacuole trafficking. *Plant Cell Physiol.* **46,** 2005–2018
41. Benfey, P. N., and Chua, N. H. (1990) The cauliflower mosaic virus 35S promoter. Combinatorial regulation of transcription in plants. *Science* **250,** 959–966
42. Cheong, Y. H., Moon, B. C., Kim, J. K., Kim, C. Y., Kim, M. C., Kim, I. H., Park, C. Y., Kim, J. C., Park, B. O., Koo, S. C., Yoon, H. W., Chung, W. S., Lim, C. O., Lee, S. Y., and Cho, M. J. (2003) BWMK1, a rice mitogen-activated protein kinase, locates in the nucleus and mediates pathogenesis-related gene expression by activation of a transcription factor. *Plant Physiol.* **132,** 1961–1972
43. Karimi, M., De Meyer, B., and Hilson, P. (2005) Modular cloning in plant cells. *Trends Plant Sci.* **10,** 103–105
44. Clough, S. J., and Bent, A. F. (1998) Floral dip. A simplified method for Agrobacterium-mediated transformation of *Arabidopsis thaliana*. *Plant J.* **16,** 735–743
45. Despres, C., Subramaniam, R., Matton, D. P., and Brisson, N. (1995) The activation of the potato PR-10a gene requires the phosphorylation of the nuclear factor PBF-1. *Plant Cell* **7,** 589–598
46. Johnson, K. D., and Bresnick, E. H. (2002) Dissecting long-range transcriptional mechanisms by chromatin immunoprecipitation. *Methods* **26,** 27–36
47. Heo, J. B., and Sung, S. (2011) Vernalization-mediated epigenetic silencing by a long intronic noncoding RNA. *Science* **331,** 76–79
48. Gendrel, A. V., Lippman, Z., Martienssen, R., and Colot, V. (2005) Profiling histone modification patterns in plants using genomic tiling microarrays. *Nat. Methods* **2,** 213–218
49. Sprang, S. R. (1997) G protein mechanisms. Insights from structural analysis. *Annu. Rev. Biochem.* **66,** 639–678
50. Barren, B., and Artemyev, N. O. (2007) Mechanisms of dominant negative G-protein α subunits. *J. Neurosci. Res.* **85,** 3505–3514
51. Noel, J. P., Hamm, H. E., and Sigler, P. B. (1993) The 2.2 Å crystal structure of transducin-α complexed with GTPγS. *Nature* **366,** 654–663
52. Nahm, M. Y., Kim, S. W., Yun, D., Lee, S. Y., Cho, M. J., and Bahk, J. D. (2003) Molecular and biochemical analyses of OsRab7, a rice Rab7 homolog. *Plant Cell Physiol.* **44,** 1341–1349
53. Wong, K. A., and Lodish, H. F. (2006) A revised model for AMP-activated protein kinase structure. The α-subunit binds to both the β- and γ-subunits although there is no direct binding between the β- and γ-subunits. *J. Biol. Chem.* **281,** 36434–36442
54. Slepak, V. Z., Katz, A., and Simon, M. I. (1995) Functional analysis of a dominant negative mutant of $G\alpha_{12}$. *J. Biol. Chem.* **270,** 4037–4041
55. Slepak, V. Z., Wilkie, T. M., and Simon, M. I. (1993) Mutational analysis of G protein α subunit G_o α expressed in *Escherichia coli*. *J. Biol. Chem.* **268,** 1414–1423
56. Swaminathan, K., Peterson, K., and Jack, T. (2008) The plant B3 superfamily. *Trends Plant Sci.* **13,** 647–655
57. Waltner, J. K., Peterson, F. C., Lytle, B. L., and Volkman, B. F. (2005) Structure of the B3 domain from *Arabidopsis thaliana* protein At1g16640. *Protein Sci.* **14,** 2478–2483
58. Levy, Y. Y., Mesnage, S., Mylne, J. S., Gendall, A. R., and Dean, C. (2002) Multiple roles of *Arabidopsis* VRN1 in vernalization and flowering time control. *Science* **297,** 243–246
59. Ratcliffe, O. J., Kumimoto, R. W., Wong, B. J., and Riechmann, J. L. (2003) Analysis of the *Arabidopsis* MADS AFFECTING FLOWERING gene family. MAF2 prevents vernalization by short periods of cold. *Plant Cell* **15,** 1159–1169
60. Chiang, G. C., Barua, D., Kramer, E. M., Amasino, R. M., and Donohue, K. (2009) Major flowering time gene, flowering locus C, regulates seed germination in *Arabidopsis thaliana*. *Proc. Natl. Acad. Sci. U.S.A.* **106,** 11661–11666
61. Eccleston, J. F., Moore, K. J., Morgan, L., Skinner, R. H., and Lowe, P. N. (1993) Kinetics of interaction between normal and proline 12 Ras and the GTPase-activating proteins, p120-GAP and neurofibromin. The significance of the intrinsic GTPase rate in determining the transforming ability of ras. *J. Biol. Chem.* **268,** 27012–27019
62. Scheffzek, K., Ahmadian, M. R., Wiesmüller, L., Kabsch, W., Stege, P., Schmitz, F., and Wittinghofer, A. (1998) Structural analysis of the GAP-related domain from neurofibromin and its implications. *EMBO J.* **17,** 4313–4327
63. Frech, M., Darden, T. A., Pedersen, L. G., Foley, C. K., Charifson, P. S., Anderson, M. W., and Wittinghofer, A. (1994) Role of glutamine 61 in the hydrolysis of GTP by p21H-ras. An experimental and theoretical study. *Biochemistry* **33,** 3237–3244
64. Landis, C. A., Masters, S. B., Spada, A., Pace, A. M., Bourne, H. R., and Vallar, L. (1989) GTPase-inhibiting mutations activate the α chain of G_s and stimulate adenylyl cyclase in human pituitary tumors. *Nature* **340,** 692–696
65. Graziano, M. P., and Gilman, A. G. (1989) Synthesis in *Escherichia coli* of GTPase-deficient mutants of G_s α. *J. Biol. Chem.* **264,** 15475–15482
66. Coleman, D. E., Berghuis, A. M., Lee, E., Linder, M. E., Gilman, A. G., and Sprang, S. R. (1994) Structures of active conformations of G_i α 1 and the mechanism of GTP hydrolysis. *Science* **265,** 1405–1412
67. Posner, B. A., Mixon, M. B., Wall, M. A., Sprang, S. R., and Gilman, A. G. (1998) The A326S mutant of $G_i\alpha$1 as an approximation of the receptor-bound state. *J. Biol. Chem.* **273,** 21752–21758
68. Reddy, V. S., and Reddy, A. S. (2004) Proteomics of calcium-signaling components in plants. *Phytochemistry* **65,** 1745–1776
69. Michaels, S. D. (2009) Flowering time regulation produces much fruit. *Curr. Opin. Plant Biol.* **12,** 75–80
70. Kotake, T., Takada, S., Nakahigashi, K., Ohto, M., and Goto, K. (2003) *Arabidopsis* TERMINAL FLOWER 2 gene encodes a heterochromatin protein 1 homolog and represses both FLOWERING LOCUS T to regulate flowering time and several floral homeotic genes. *Plant Cell Physiol.* **44,** 555–564
71. Giraudat, J., Hauge, B. M., Valon, C., Smalle, J., Parcy, F., and Goodman, H. M. (1992) Isolation of the *Arabidopsis* ABI3 gene by positional cloning. *Plant Cell* **4,** 1251–1261
72. Ulmasov, T., Hagen, G., and Guilfoyle, T. J. (1997) ARF1, a transcription factor that binds to auxin response elements. *Science* **276,** 1865–1868
73. Kagaya, Y., Ohmiya, K., and Hattori, T. (1999) RAV1, a novel DNA-binding protein, binds to bipartite recognition sequence through two distinct DNA-binding domains uniquely found in higher plants. *Nucleic Acids Res.* **27,** 470–478
74. Love, J., Dodd, A. N., and Webb, A. A. (2004) Circadian and diurnal calcium oscillations encode photoperiodic information in *Arabidopsis*. *Plant Cell* **16,** 956–966
75. Imaizumi, T., Schroeder, J. I., and Kay, S. A. (2007) In SYNC. The ins and outs of circadian oscillations in calcium. *Sci. STKE* **2007,** pe32